Author(s): Bree, N.; Wrzosek-Lipska, K.; Petts, A.; Andreyev, A.; Bastin, B.; Bender, M.; Blazhev, A.; Bruyneel, B.; Butler, P. A.; Butterworth, J.; Carpenter, M. P.; Cederkäll, J.; Clément, E.; Cocolios, T. E.; Deacon, A.; Diriken, J.; Ekström, A.; Fitzpatrick, C.; Fraile, L. M.; Fransen, Ch.; Freeman, S. J.; Gaffney, L. P.; García-Ramos, J. E.; Geibel, K.; Gernhäuser, R.; Grahn, Tuomas; Guttormsen, M.; Hadinia, B.; Hadyńska-Kle¸k, K.; Hass, M.;

Title: Shape Coexistence in the Neutron-Deficient Even-Even Hg182−188 Isotopes Studied via Coulomb Excitation

Year: 2014

Version:

Please cite the original version:

Bree, N., Wrzosek-Lipska, K., Petts, A., Andreyev, A., Bastin, B., Bender, M., Blazhev, A., Bruyneel, B., Butler, P. A., Butterworth, J., Carpenter, M. P., Cederkäll, J., Clément, E., Cocolios, T. E., Deacon, A., Diriken, J., Ekström, A., Fitzpatrick, C., Fraile, L. M., . . . Zielińska, A. M. (2014). Shape Coexistence in the Neutron-Deficient Even-Even Hg182−188 Isotopes Studied via Coulomb Excitation. Physical Review Letters, 112(16), 162701. https://doi.org/10.1103/PhysRevLett.112.162701

Shape Coexistence in the Neutron-Deficient Even-Even $^{182-188}$Hg Isotopes Studied via Coulomb Excitation

N. Bree,[1] K. Wrzosek-Lipska,[1,2,*] A. Petts,[3] A. Andreyev,[1,4] B. Bastin,[1,5] M. Bender,[6,7] A. Blazhev,[8] B. Bruyneel,[8] P. A. Butler,[3] J. Butterworth,[4] M. P. Carpenter,[9] J. Cederkäll,[10,11] E. Clément,[5,11] T. E. Cocolios,[1,11,12] A. Deacon,[12] J. Diriken,[1,13] A. Ekström,[10] C. Fitzpatrick,[12] L. M. Fraile,[11,14] Ch. Fransen,[8] S. J. Freeman,[12] L. P. Gaffney,[1,3] J. E. García-Ramos,[15] K. Geibel,[8] R. Gernhäuser,[16] T. Grahn,[17,18] M. Guttormsen,[19] B. Hadinia,[20,21] K. Hadyńska-Klęk,[2] M. Hass,[22] P.-H. Heenen,[23] R.-D. Herzberg,[3] H. Hess,[8] K. Heyde,[24] M. Huyse,[1] O. Ivanov,[1] D. G. Jenkins,[4] R. Julin,[17] N. Kesteloot,[1,13] Th. Kröll,[25] R. Krücken,[16] A. C. Larsen,[19] R. Lutter,[26] P. Marley,[4] P. J. Napiorkowski,[2] R. Orlandi,[1,20] R. D. Page,[3] J. Pakarinen,[17,18] N. Patronis,[1,27] P. J. Peura,[17] E. Piselli,[11] P. Rahkila,[17] E. Rapisarda,[11] P. Reiter,[8] A. P. Robinson,[4,12] M. Scheck,[3,20,28] S. Siem,[19] K. Singh Chakkal,[22] J. F. Smith,[20] J. Srebrny,[2] I. Stefanescu,[1,16] G. M. Tveten,[19] P. Van Duppen,[1] J. Van de Walle,[11] D. Voulot,[11] N. Warr,[8] F. Wenander,[11] A. Wiens,[8] J. L. Wood,[29] and M. Zielińska[2,30]

[1]*KU Leuven, Instituut voor Kern- en Stralingsfysica, B-3001 Leuven, Belgium*
[2]*Heavy Ion Laboratory, University of Warsaw, PL-02-093 Warsaw, Poland*
[3]*Oliver Lodge Laboratory, University of Liverpool, Liverpool L69 7ZE, United Kingdom*
[4]*Department of Physics, University of York, York YO10 5DD, United Kingdom*
[5]*GANIL CEA/DSM-CNRS/IN2P3, Boulevard H. Becquerel, F-14076 Caen, France*
[6]*Université Bordeaux, Centre d'Etudes Nucléaires de Bordeaux Gradignan, UMR5797, F-33175 Gradignan, France*
[7]*CNRS/IN2P3, Centre d'Etudes Nucléaires de Bordeaux Gradignan, UMR5797, F-33175 Gradignan, France*
[8]*Institut für Kernphysik, Universität zu Köln, 50937 Köln, Germany*
[9]*Physics Division, Argonne National Laboratory, Argonne, Illinois 60439, USA*
[10]*Physics Department, University of Lund, Box 118, SE-221 00 Lund, Sweden*
[11]*ISOLDE, CERN, CH-1211 Geneva 23, Switzerland*
[12]*School of Physics and Astronomy, University of Manchester, Manchester M13 9PL, United Kingdom*
[13]*Belgian Nuclear Research Centre SCK CEN, B-2400 Mol, Belgium*
[14]*Grupo de Física Nuclear, Universidad Complutense de Madrit, 28040 Madrid, Spain*
[15]*Departamento de Física Aplicada, Universidad de Huelva, 21071 Huelva, Spain*
[16]*Physics Department E12, Technische Universität München, D-85748 Garching, Germany*
[17]*Department of Physics, University of Jyväskylä, P.O. Box 35, FI-40014 Jyväskylä, Finland*
[18]*Helsinki Institute of Physics, University of Helsinki, P.O. Box 64, FIN-00014 Helsinki, Finland*
[19]*Department of Physics, University of Oslo, N-0316 Oslo, Norway*
[20]*School of Engineering, University of the West of Scotland, Paisley PA1 2BE, United Kingdom*
[21]*Department of Physics, University of Guelph, Guelph, Ontario N1G 2W1, Canada*
[22]*Department of Particle Physics, Weizmann Institute of Science, Rehovot 76100, Israel*
[23]*Physique Nucléaire Théorique, Université Libre de Bruxelles, B-1050 Bruxelles, Belgium*
[24]*Department of Physics and Astronomy, Ghent University, B-9000 Gent, Belgium*
[25]*Institut für Kernphysik, Technische Universität Darmstadt, D-64289 Darmstadt, Germany*
[26]*Department of Physics, Ludwig Maximilian Universität München, 85748 Garching, Germany*
[27]*Department of Physics, The University of Ioannina, GR-45110 Ioannina, Greece*
[28]*SUPA, Scottisch Universities Physics Alliance, Glasgow G12 8QQ, United Kingdom*
[29]*School of Physics, Georgia Institute of Technology, Atlanta, Georgia 30332-0430, USA*
[30]*IRFU/SPhN, CEA Saclay, F-91191 Gif-sur-Yvette, France*

(Received 8 November 2013; revised manuscript received 14 February 2014; published 23 April 2014)

Coulomb-excitation experiments to study electromagnetic properties of radioactive even-even Hg isotopes were performed with 2.85 MeV/nucleon mercury beams from REX-ISOLDE. Magnitudes and relative signs of the reduced $E2$ matrix elements that couple the ground state and low-lying excited states in $^{182-188}$Hg were extracted. Information on the deformation of the ground and the first excited 0^+ states was deduced using the quadrupole sum rules approach. Results show that the ground state is slightly deformed and of oblate nature, while a larger deformation for the excited 0^+ state was noted in ^{182,184}Hg. The results are compared to beyond mean field and interacting-boson based models and interpreted within a two-state mixing model. Partial agreement with the model calculations was obtained. The presence of two different structures in the light even-mass mercury isotopes that coexist at low excitation energy is firmly established.

DOI: 10.1103/PhysRevLett.112.162701 PACS numbers: 25.70.De, 23.20.Lv, 23.20.-g, 25.60.-t

Shape coexistence, whereby at low energy near-degenerate states characterized by different shapes appear, is an intriguing phenomenon that occurs in various mesoscopic systems. However, the distinctive character of shape coexistence in atomic nuclei lies in the subtle interplay between two opposing trends [1]. Shell and subshell closures invoke a stabilizing effect leading to sphericity while residual interactions between protons and neutrons outside closed shells drive the nucleus to deformation. Understanding the manifestation of shape coexistence could be the key to reveal the microscopic origin of collectivity and the apparent evaporation of the shell structure in atomic nuclei. In the region around the light lead isotopes, with proton number $Z = 82$, a substantial amount of information has been collected using a wide spectrum of experimental probes such as decay studies, optical spectroscopy studies, and in-beam spectroscopy investigations [1,2]. This resulted, amongst other things, in the observation of strong staggering in the isotope shifts in the mercury isotopes [3], the discovery of triple shape coexistence in ^{186}Pb [4], and an early onset of deformation in the light polonium and platinum isotopes as evidenced through laser spectroscopy (see, e.g., [5]). The global trends of these experimental findings are reproduced by theoretical descriptions, such as phenomenological shape-mixing calculations and contemporary symmetry-guided models (e.g., [6,7]), and beyond mean-field approaches [5,8,9]. However, there is a lack of direct experimental information on the nature of the quadrupole deformation or on the mixing of the states belonging to the coexisting structures.

The energy-level systematics of the even-even mercury isotopes ranging from $A = 190$ to $A = 198$ exhibit a nearly constant behavior of the energy of the yrast states [2,10]. Mean-field calculations suggested that these states are related to a weakly deformed oblate ground state [1,8,9]. For the lighter, neutron-deficient mercury isotopes ($A \leq 186$), this pattern is distorted through the appearance of more deformed states, interpreted to be prolate, which decrease in excitation energy, reaching a minimum around the neutron midshell ($N = 104$, ^{184}Hg), and mix with the weakly deformed states. However, as shown by the mean-square charge radius measurements [11], it appears that mixing in the ground states is small (see, e.g., [5]).

In spite of this distortion, the energy of the 2_1^+ state of even-even Hg isotopes around the $N = 104$ midshell is relatively constant. Moreover, recent lifetime measurements for the yrast states reveal comparable values of the reduced transition probabilities, $B(E2; 2_1^+ \rightarrow 0_1^+)$, for even-even $^{182-188}$Hg isotopes [12–14]. On the other hand, strong conversion of $2_2^+ \rightarrow 2_1^+$ transitions associated with an $E0$ component have been observed [15,16], indicating mixing of these states. In order to resolve these apparently contradictory observations and to obtain information on the mixing and the type of deformation, the electromagnetic properties of low-lying yrast and non-yrast states in $^{182-188}$Hg have to be determined. While Coulomb excitation is the preferred probe, energetic radioactive beams are required in this case.

Coulomb excitation of even-even $^{182-188}$Hg was carried out at the REX-ISOLDE facility at CERN [17,18]. A radioactive mercury-ion beam was accelerated to an energy of 2.85 MeV/nucleon and delivered to the MINIBALL setup [19]. Coulomb excitation of $^{182-188}$Hg was induced by ^{120}Sn, ^{107}Ag, and ^{112,114}Cd targets of thicknesses of 2.3, 1.1, and 2 mg/cm^2, respectively. The beam intensity varied between 3.5×10^3 pps up to 0.2–2.0×10^5 pps for ^{182}Hg and $^{184-188}$Hg, respectively. The experimental setup consisted of the MINIBALL γ-ray spectrometer coupled with the double-sided silicon strip detector (DSSSD) [19,20].

The low-energy states in $^{182-188}$Hg that were populated in the experiment are presented in Fig. 1. A random-subtracted, γ-ray spectrum of a ^{182}Hg beam incident on a ^{112}Cd target, in coincidence with both projectile and target particles and Doppler corrected for a projectile, is presented in Fig. 2. The population of the 2_1^+, 2_2^+, and 4_1^+ states in ^{182}Hg can be clearly observed. Moreover, intense K x-ray peaks are present in the spectrum. A careful analysis of these peaks, that were Doppler broadened, reveals that they stem partly from x rays produced in atomic process when the ^{182}Hg ions pass the target and partly from electron conversion accompanying the observed γ-ray transitions

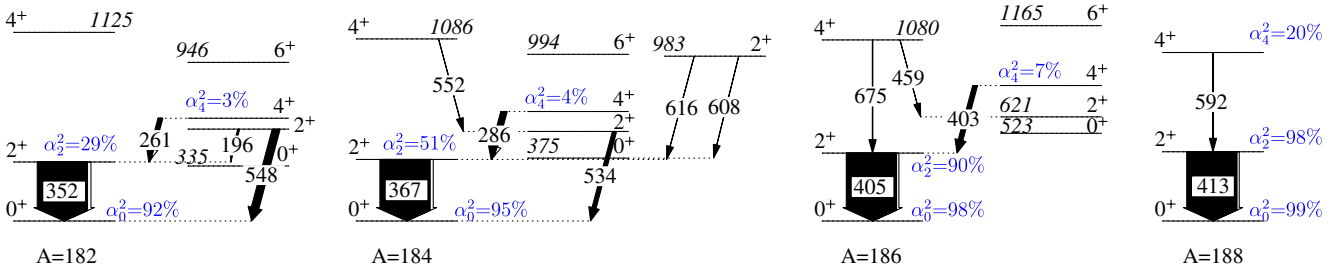

FIG. 1 (color online). Low-energy part of the level schemes, relevant to the Coulomb-excitation analysis, of the even-even $^{182-188}$Hg isotopes. Level and γ-ray transition energies are given in keV. Widths of the arrows are proportional to the observed γ-ray yields normalized to the $2_1^+ \rightarrow 0_1^+$ transition. The intensity of the $2_2^+ \rightarrow 2_1^+$ transition in ^{182}Hg, not visible in the spectrum in Fig. 2 due to the presence of Compton edge of $2_1^+ \rightarrow 0_1^+$ transition, was deduced from the $\gamma - \gamma$ ray spectrum gated on the $2_1^+ \rightarrow 0_1^+$ peak. Mixing amplitudes squared of the unperturbed structure (I), α_J^2, are taken from [14].

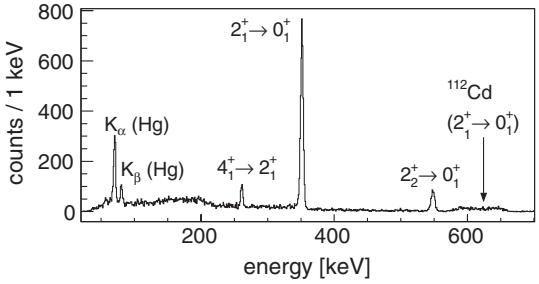

FIG. 2. Random-subtracted γ-ray spectrum of ^{182}Hg Coulomb excited by a ^{112}Cd target, Doppler corrected for the projectile. Intense K x-ray peaks are clearly visible in the spectrum.

and the deexcitation of the 0_2^+ state to the ground state [21]. From their intensities, the population of the 0_2^+ excited state was deduced and information on all connecting $E2$ matrix elements ($ME2$'s) was obtained, albeit with limited precision. Data of similar quality were collected for ^{184,186,188}Hg. Crucial for this analysis was the knowledge of the conversion coefficient of the $2_2^+ \rightarrow 2_1^+$ transition, as it contained a large $E0$ component. The total conversion coefficient, $\alpha(2_2^+ \rightarrow 2_1^+)$, deduced from the β-decay studies of ^{182,184}Tl, is equal to 4.7 ± 1.3 in ^{182}Hg and 23 ± 5 in ^{184}Hg [15].

In order to determine $ME2$'s in $^{182-188}$Hg, the Coulomb-excitation least-squares fitting code GOSIA [22] was used. The code fits a set of reduced matrix elements to reproduce the measured yield of γ-ray transitions depopulating the Coulomb-excited states of $^{182-188}$Hg, taking into account known spectroscopic data related to electromagnetic matrix elements: branching ratios [15,23,24], conversion coefficients [15,25], and lifetimes of the yrast and non-yrast states [13,14,26]. Importantly, for all cases, the fitted $B(E2; 2_1^+ \rightarrow 0_1^+)$ values obtained without lifetimes as additional data are consistent with results reported in Refs. [12–14].

The analysis of the Coulomb-excitation data brings information on the relative signs of transition $ME2$'s. The absolute sign of a single, transition $ME2$ has no physical meaning, since it depends on the arbitrary choice of the relative phases of a wave function of initial and final states. However, the sign of the product—the interference term, e.g., $\langle 0_1^+ \| E2 \| 2_1^+ \rangle \langle 2_1^+ \| E2 \| 2_2^+ \rangle \langle 2_2^+ \| E2 \| 0_1^+ \rangle$—is independent of the chosen convention and can be determined experimentally since it influences the Coulomb-excitation cross section.

The extracted $ME2$'s are shown in Table I. These results can be analyzed in terms of the quadrupole deformation parameters, Q and δ, which are universal variables of quadrupole collective models within the General Bohr Hamiltonian (GBH) [27]. Using the quadrupole sum rules approach [28–31] the quadrupole invariants, $\langle Q^2 \rangle$ and $\langle Q^3 \cos(3\delta) \rangle$, can then be obtained. Invariants describe the charge distribution of a nucleus in a given nuclear state. The sums of products of the relevant $ME2$'s between 0^+ and 2^+ states given in Table I are shown in Fig. 3: the sum

TABLE I. Reduced transitional and diagonal $E2$ matrix elements between low-lying states in $^{182-188}$Hg obtained in this work. The error bars correspond to 1σ. The ($\pm$) indicates that the sign of the $\langle 0_1^+ \| E2 \| 2_2^+ \rangle$ for ^{186}Hg was not determined.

$\langle I_i \| E2 \| I_f \rangle$ (eb)	^{182}Hg	^{184}Hg	^{186}Hg	^{188}Hg
$\langle 0_1^+ \| E2 \| 2_1^+ \rangle$	$1.29^{+0.04}_{-0.03}$	1.27 (3)	$1.25^{+0.10}_{-0.07}$	1.31 (10)
$\langle 2_1^+ \| E2 \| 4_1^+ \rangle$	3.71 (6)	3.15 (6)	3.4 (2)	2.07(8)
$\langle 0_1^+ \| E2 \| 2_2^+ \rangle$	−0.61 (3)	0.21 (2)	($\pm$) 0.05 (1)	
$\langle 0_2^+ \| E2 \| 2_1^+ \rangle$	$-2.68^{+0.15}_{-0.13}$	3.3 (8)		
$\langle 0_2^+ \| E2 \| 2_2^+ \rangle$	−1.7 (2)	1.25 (28)	$\geq$ 3.7 (8)	
$\langle 2_1^+ \| E2 \| 2_2^+ \rangle$	−2.2 (4)	0.91 (14)		
$\langle 2_2^+ \| E2 \| 4_1^+ \rangle$	3.1 (3)	5.8 (5)	$-5.3^{+1.3}_{-0.5}$	
$\langle 2_1^+ \| E2 \| 2_1^+ \rangle$	$-0.04^{+1.30}_{-1.40}$	$1.5^{+1.8}_{-1.2}$		$1.0^{+0.6}_{-0.4}$
$\langle 2_2^+ \| E2 \| 2_2^+ \rangle$	$0.8^{+1.0}_{-0.6}$	−2.6 (20)		

of squared $E2$ matrix elements (SSM) related to $\langle Q^2 \rangle$ and the sum of triple products of $E2$ matrix elements (STM) related to $\langle Q^3 \cos(3\delta) \rangle$. The quadrupole invariants can be further related to the GBH collective model variables [31], β (overall deformation parameter) and γ (nonaxiality parameter). It can be concluded that the ground states of the even-even mercury isotopes are weakly deformed with a β value close to 0.15 and are consistent with an oblatelike deformation [$\langle \cos(3\delta) \rangle \simeq -1$], while the excited 0^+ states are more deformed. The lack of precision on key matrix elements, especially in ^{186,188}Hg, prevents us from drawing firm conclusions on the nature of the deformation of the ground (^{186}Hg) or excited (^{186,188}Hg) 0^+ states.

Sums of the products of the relevant $ME2$'s given in Table I, were compared to the equivalent sums (including to the 2_2^+ state) calculated from beyond mean field (BMF) [9] and interacting boson-based models (IBM) [32] (Fig. 3). The BMF excitation spectrum of neutron-deficient Hg isotopes is dominated by two coexisting rotational bands

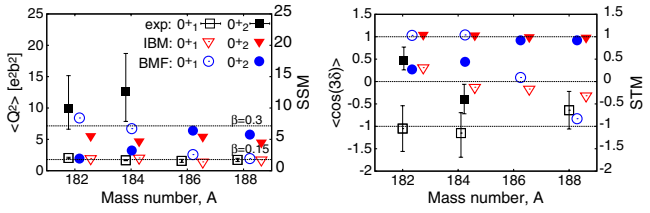

FIG. 3 (color online). The SSM and STM values of the 0_1^+ (open symbols) and 0_2^+ (full symbols) extracted from the $ME2$'s obtained in this work (black squares) are compared to the equivalent values from the BMF (blue circles) and IBM (red triangles) calculations. The ^{188}Hg experimental data points represent only contributions to the 2_1^+ state. Within the quadrupole collective models these can be related to the quadrupole invariants ($\langle Q^2 \rangle$ and $\langle \cos(3\delta) \rangle$ representing the overall deformation and the axial asymmetry, respectively) as well as the β and γ parameters through the GBH model. To maintain clarity, some markers are slightly offset from integer values.

with very different moments of inertia. In the BMF calculation, when going to the lighter masses, these two bands cross, in contradiction with experiment. Down to $N = 106$, the BMF Hg ground states are predicted to be predominantly oblate and the first excited 0_2^+ state to be prolate, whereas for $100 \leq N \leq 104$, the ground state is predominantly prolate and the 0_2^+ state is an almost equal mixture of prolate and oblate configurations [9]. The sums of products of the relevant $ME2$'s from the BMF calculations, SSM and STM, take values that reflect this behavior. As can be seen in the left part of Fig. 3 the SSM sum for the 0^+ ground states deduced from BMF $ME2$'s values agree with data for $A = 186$ and 188. By contrast, for $A = 182$ and 184, the BMF SSM values for the ground state and the second 0^+ are inverted with respect to experiment. This disagreement is also visible in the STM values plotted in the right panel of Fig. 3.

In the IBM approach [32], whereby particle-hole pair excitations across the $Z = 82$ closed shell are explicitly included (for a similar calculation see, e.g., [6,33]), agreement between experiment and calculations for the SSM sum is noticed. However, as in the case of the BMF calculations, only partial agreement between experiment and theory is observed for the sum of triple product of IBM $ME2$'s. The disagreements for the two models are not understood and point to missing ingredients in the calculations. This is further addressed in [32].

The assumption that the excited states of the mercury isotopes can be described by two distinct configurations can also be tested by comparing our results with those from a two-state mixing model. Within this simple, phenomenological approach, following the notation given in Refs. [34,35], the observed physical states can be written as linear combinations of two unmixed structures—structure I and structure II—with specific mixing amplitudes.

The experimental (mixed) $ME2$'s can be expressed in terms of the pure intraband matrix elements which couple unperturbed states and of the mixing amplitudes. It is assumed that there are no interband unperturbed transitions between the two pure structures. The mixing probabilities, taken from Ref. [14] and reproduced in Fig. 1, were derived from the fit of known, higher-lying level energies of rotational bands, built upon the first two 0^+ states, using the variable moment of inertia (VMI) model [36].

All matrix elements within the unperturbed bands ($ME2$'s between 0^+ and 2^+ as well as spectroscopic moments of the 2^+'s) were fitted as a common set for $^{182-188}$Hg to optimally reproduce experimental results. This yields 1.2 and 3.3 eb values for the $\langle 0_{\rm I}^+ \| E2 \| 2_{\rm I}^+ \rangle$ and $\langle 0_{\rm II}^+ \| E2 \| 2_{\rm II}^+ \rangle$, respectively, while the diagonal matrix elements for the $2_{\rm I}^+$ and $2_{\rm II}^+$ states result in 1.8 and -4.0 eb, respectively. To derive mixed $ME2$'s connecting 4^+ and 2^+ states, the unperturbed $\langle 2_{\rm I(II)}^+ \| E2 \| 4_{\rm I(II)}^+ \rangle$ matrix elements were extrapolated from the $\langle 0_{\rm I(II)}^+ \| E2 \| 2_{\rm I(II)}^+ \rangle$ values using the rotational formula [37] and are equal to 1.9 and 5.3 eb, respectively. Figure 4 shows a comparison between the experimental transition $ME2$'s and those resulting from the two-state mixing model.

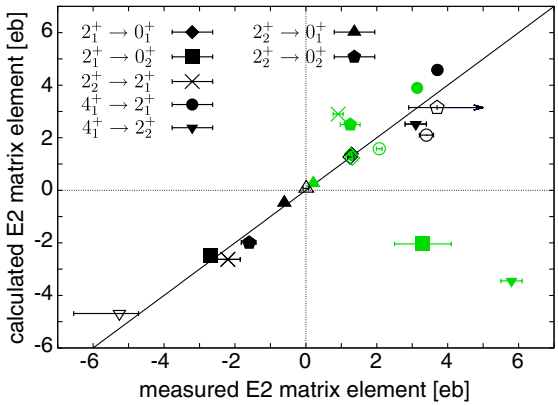

FIG. 4 (color online). The $ME2$'s obtained in this work, compared to those extracted from the two-state mixing calculations for ^{182}Hg (full black and cross), ^{184}Hg [full green (light grey) and cross], ^{186}Hg (open black) and ^{188}Hg [open green (light grey)].

Most of the experimental results are well reproduced within the two-state mixing model supporting the interpretation of two unperturbed sets of states that mix when states with equal spin and parity are close in energy. Reduced transition probabilities between 2^+ and 0^+ states, extracted in this work, belonging to two pure structures are significantly different [the $B(E2; 2_{\rm II}^+ \to 0_{\rm II}^+)$ value is 7.5 times larger than the $B(E2; 2_{\rm I}^+ \to 0_{\rm I}^+)$] hinting towards different magnitudes of quadrupole collectivity, consistent with the conclusions discussed above (Fig. 3). Moreover, within the collective models (e.g., Bohr-Mottelson model [37]) when two bands are described by the same K quantum number, an opposite sign of the diagonal matrix elements of the $2_{\rm I}^+$ and $2_{\rm II}^+$ states indicates a change in the type of deformation for the two configurations—less deformed and of oblate nature (structure I) and more deformed and of prolate nature (structure II).

The near-constant excitation energy of the 2_1^+ state and of the $\langle 0_1^+ \| E2 \| 2_1^+ \rangle$ value can now be explained within the two-state mixing model in spite of a substantial change in the mixing amplitude $\alpha_{J=2}$. The 2_1^+ states change from a rather pure component of structure I (for ^{188}Hg) into a state with a dominant component of structure II in ^{182}Hg. The small mixing in the 0^+ ground states compensates for this effect as can be observed from the $\langle 2_2^+ \| E2 \| 0_1^+ \rangle$ (see Fig. 4).

The predictions of the two-level mixing model deviate partially from the experimental results obtained for ^{184}Hg, where approximately 50% of mixing between 2_1^+ and 2_2^+ states was deduced [14]. While the absolute values of most matrix elements are in reasonable agreement, the signs are not. The influence of variations of the mixing amplitudes within 20% has been investigated, but did not cure this discrepancy.

In conclusion, the electromagnetic properties of low-lying states of light, even-mass neutron-deficient $^{182-188}$Hg

were studied through Coulomb excitation using postaccelerated radioactive-ion beams. Combining these experimental data with results from β-decay studies of ^{182,184}Tl [15] and lifetime measurements [12–14,26] yielded a unique set of $ME2$'s between yrast and non-yrast 0^+, 2^+, and 4^+ states including their relative signs. This enabled us to use the quadrupole sum rules to analyze the quadrupole collectivity of the ground and excited 0^+ states of $^{182-188}$Hg. It shows that the ground states of mercury isotopes are weakly deformed and of predominantly oblate nature, while the excited 0^+ states of ^{182,184}Hg are more deformed. Comparison of sums of squared M$E2$'s (SSM) shows agreement with IBM calculations and partial agreement with BMF predictions.

Properties of the lowest-lying states of $^{182-188}$Hg were interpreted within a two-state mixing model. It was shown that the magnitudes of most of the experimentally determined transition M$E2$'s can be explained in terms of mixing of two significantly different configurations. The unmixed matrix elements extrapolated from our data, using the VMI model, towards higher-lying states, where no mixing occurs, are in a fair agreement with the theoretical predictions and lifetime measurements [12,14]. These findings support the underlying assumption of two different structures that are pure at higher spin values and mix at low excitation energy. For these light mercury isotopes, the new data imply significant changes in the composition of the 2_1^+ states via large variations in the deduced mixing amplitudes. This refutes the common interpretation according to which states, in an isotopic chain, of comparable energy and similar transition strength always manifest a similar structure.

The authors would like to thank the ISOLDE facility for providing excellent beams. This work was supported by the FWO-Vlaanderen (Belgium), an FWO Pegasus Marie Curie Fellowship (L. P. G.), by GOA/2010/010 (BOF KULeuven), by the IAP Belgian Science Policy (BriX network P6/23 and P7/12), by the European Commission within the 7th Framework Programme through I3-ENSAR (Contract No. RII3-CT-2010-262010), by the U.K. Science and Technology Facilities Council, by the German BMBF under Contracts No. 06DA9036I, No. 05P12RDCIA, No. 06KY205I, No. 05P09PKCI5, No. 05P12PKFNE, No. 05P12WOFNF, and No. 09MT9156, Academy of Finland (Contract No. 131665), by the Spanish MINECO through FPA2010-17142 project and the Spanish Project No. FIS2011-28738-C02-02.

*Corresponding author.
kasia.wrzoseklipska@fys.kuleuven.be

[1] K. Heyde and J. L. Wood, Rev. Mod. Phys. **83**, 1467 (2011).
[2] R. Julin, K. Helariutta, and M. Muikku, J. Phys. G **27**, R109 (2001).
[3] G. Ulm *et al.*, Z. Phys. A **325**, 247 (1986).
[4] A. N. Andreyev *et al.*, Nature (London) **405**, 430 (2000).
[5] T. E. Cocolios *et al.*, Phys. Rev. Lett. **106**, 052503 (2011).
[6] J. E. García-Ramos, V. Hellemans, and K. Heyde, Phys. Rev. C **84**, 014331 (2011).
[7] K. Nomura, R. Rodriguez-Guzman, and L. M. Robledo, Phys. Rev. C **87**, 064313 (2013).
[8] M. Bender, P.-H. Heenen, and P.-G. Reinhard, Rev. Mod. Phys. **75**, 121 (2003).
[9] J. M. Yao, M. Bender, and P. H. Heenen, Phys. Rev. C **87**, 034322 (2013).
[10] J. Elseviers *et al.*, Phys. Rev. C **84**, 034307 (2011).
[11] J. Bonn, G. Huber, H.-J. Kluge, L. Kugler, and E. W. Otten, Phys. Lett. **38B**, 308 (1972).
[12] T. Grahn *et al.*, Phys. Rev. C **80**, 014324 (2009).
[13] M. Scheck *et al.*, Phys. Rev. C **81**, 014310 (2010).
[14] L. P. Gaffney *et al.*, Phys. Rev. C **89**, 024307 (2014).
[15] E. Rapisarda *et al.* (to be published).
[16] M. Scheck *et al.*, Phys. Rev. C **83**, 037303 (2011).
[17] D. Habs *et al.*, Nucl. Instrum. Methods Phys. Res., Sect. B **139**, 128 (1998).
[18] O. Kester *et al.*, Nucl. Instrum. Methods Phys. Res., Sect. B **204**, 20 (2003).
[19] N. Warr *et al.*, Eur. Phys. J. A **49**, 40 (2013).
[20] A. N Ostrowski, S. Cherubini, T. Davinson, D. Groombridge, A. M. Laird, A. Musumarra, A. Ninane, A. di Pietro, A. C. Shotter, and P. J. Woods, Nucl. Instrum. Methods Phys. Res., Sect. A **480**, 448 (2002).
[21] N. Bree *et al.* (to be published).
[22] T. Czosnyka, D. Cline, and C. Y. Wu, Bull. Am. Phys. Soc. **28**, 745 (1982).
[23] J. D. Cole *et al.*, Phys. Rev. C **16**, 2010 (1977).
[24] R. Béraud, M. Meyer, M. G. Desthuilliers, C. Bourgeois, P. Kilcher, and J. Letessier, Nucl. Phys. **A284**, 221 (1977).
[25] T. Kibédi, T. W. Burrows, M. B. Trzhaskovskaya, P. M. Davidson, and C. W. Nestor, Nucl. Instrum. Methods Phys. Res., Sect. A **589**, 202 (2008).
[26] P. K. Joshi *et al.*, Int. J. Mod. Phys. E **03**, 757 (1994).
[27] L. Próchniak and G. Rohoziński, J. Phys. G **36**, 123101 (2009).
[28] K. Kumar, Phys. Rev. Lett. **28**, 249 (1972).
[29] D. Cline, Annu. Rev. Nucl. Part. Sci. **36**, 683 (1986).
[30] J. Srebrny and D. Cline, Int. J. Mod. Phys. E **20**, 422 (2011), and references therein.
[31] K. Wrzosek-Lipska *et al.*, Phys. Rev. C **86**, 064305 (2012).
[32] J. E. García-Ramos and K. Heyde, Phys. Rev. C **89**, 014306 (2014).
[33] J. E. García-Ramos and K. Heyde, Nucl. Phys. **A825**, 39 (2009).
[34] P. Brussaard and P. W. M. Glaudemans, *Shell-Model Applications in Nuclear Spectroscopy* (North-Holland, Dordrecht, 1977).
[35] P. Van Duppen, M. Huyse, and J. L. Wood, J. Phys. G **16**, 441 (1990).
[36] M. A. J. Mariscotti, G. Scharff-Goldhaber, and B. Buck, Phys. Rev. **178**, 1864 (1969).
[37] A. Bohr and B. R. Mottelson, *Nuclear Structure* (Benjamin, Inc., New York, 1969), Vol. II.